Earth and Planetary Science Letters 284 (2009) 124–131

Contents lists available at ScienceDirect

Earth and Planetary Science Letters

journal homepage: www.elsevier.com/locate/epsl

Self-reversal and apparent magnetic excursions in Arctic sediments

J.E.T. Channell *, C. Xuan

Department of Geological Sciences, University of Florida, 241 Williamson Hall, POB 112120, Gainesville, FL 32611, United States

ARTICLE INFO

Article history:
Received 2 September 2008
Received in revised form 17 March 2009
Accepted 15 April 2009
Available online 13 May 2009
Editor: P. DeMenocal

Keywords:
Arctic sediments
geomagnetic excursions
titanomaghemite
self-reversal

ABSTRACT

The Arctic oceans have been fertile ground for the recording of apparent excursions of the geomagnetic field, implying that the high latitude field had unusual characteristics at least over the last 1–2 Myrs. Alternating field demagnetization of the natural remanent magnetization (NRM) of Core HLY0503-6JPC from the Mendeleev Ridge (Arctic Ocean) implies the presence of primary magnetizations with negative inclination apparently recording excursions in sediments deposited during the Brunhes Chron. Thermal demagnetization, on the other hand, indicates the presence of multiple (often anti-parallel) magnetization components with negative inclination components having blocking temperatures predominantly, but not entirely, below ~350 °C. Thermo-magnetic tests, X-ray diffraction (XRD) and scanning electron microscopy (SEM) indicate that the negative inclination components are carried by titanomaghemite, presumably formed by seafloor oxidation of titanomagnetite. The titanomaghemite apparently carries a chemical remanent magnetization (CRM) that is partially self-reversed relative to the detrital remanent magnetization (DRM) carried by the host titanomagnetite. The partial self-reversal could have been accomplished by ionic ordering during oxidation, thereby changing the balance of the magnetic moments in the ferrimagnetic sublattices.

1. Introduction

Piston cores from the Arctic and Norwegian–Greenland Sea have presented a stratigraphic challenge due to the lack of biogenic carbonate (foraminifera) for isotope analyses and poorly constrained biostratigraphies. As explained by Backman et al. (2004), the Arctic Ocean was considered a sediment starved basin with mm/kyr scale sedimentation rates based largely on the interpretation of magnetostratigraphic records in which the Matuyama–Brunhes boundary was often placed ~1 m below seafloor (e.g., Steuerwald et al., 1968; Clark, 1970). Since the 1980s, higher (cm/kyr scale) sedimentation rates have become evident throughout the Arctic oceans from radiocarbon dates, and biostratigraphic observations (e.g., Markussen et al., 1985). These revised ages resulted in radical change in magnetostratigraphic interpretations, with records from the Arctic Ocean and Norwegian–Greenland Sea being interpreted to exhibit intervals of negative inclination (excursions) within the Brunhes Chron (Løvlie et al., 1986; Bleil and Gard, 1989; Nowaczyk and Baumann, 1992; Nowaczyk et al., 1994; Nowaczyk and Antonow, 1997; Nowaczyk and Knies, 2000). Excursion ages, derived from outside the Arctic, have then been adopted as age control points in Arctic cores. The paucity of corroborating stratigraphic information in the Arctic and Norwegian–Greenland Sea results in a high degree of freedom in labeling the apparent magnetic excursions.

In 2004, the Integrated Ocean Drilling Program (IODP) Arctic Coring Expedition (ACEX) focused the resources of IODP on drilling on the crest of the Lomonosov Ridge (Fig. 1) (Backman et al., 2006). In a recent ACEX age model (Backman et al., 2008), the authors broke with tradition and constructed their age model without using paleomagnetic data, apart from one (Paleocene) polarity reversal. Backman et al. (2008) were circumspect about the magnetic data and concluded that: "the occurrence of these high frequency polarity changes in the Neogene ACEX sediment sequence may represent either distortions of the paleomagnetic record, or the genuine behavior of the geomagnetic field in this part of the Arctic Ocean". The ACEX NRM inclination record (after 40 mT peak field demagnetization) indicates an upper 4.6 m of predominantly steep positive inclinations interspersed with few cm-scale events where the inclination values are negative (O'Regan et al., 2008). The few cm thick events were correlated to the Mono Lake excursion (~33 ka), the Laschamp excursion (~41 ka), and the Norwegian–Greenland Sea excursions at 55 and 66 ka. These age assignments are consistent with four radiocarbon ages and the presence of a few specimens of *E. huxleyi* at 1.91 mcd (meters composite depth), interpreted as indicative of MIS5 (Cronin et al., 2008). Below this uppermost 4.6 m interval, well-defined zones of steep positive and steep negative inclinations are interspersed, with the uppermost negative inclination interval associated with the Biwa II magnetic excursion at ~240 ka (O'Regan et al., 2008). In comparing the ACEX inclination record below ~4.6 m depth with the inclination record in neighboring Cores PS-2186-6 and 96/12-1PC, O'Regan et al. (2008) state: "the overall similarity in the excursion patterns at these and other Arctic sites suggests they record synchronous variations in the global dipole field. However, once these cores have been stratigraphically aligned using sediment physical properties, it becomes apparent that inclination changes are not necessarily synchronous".

* Corresponding author. Tel.: + 352 392 3658; fax: +1 352 392 9294.
E-mail addresses: jetc@geology.ufl.edu (J.E.T. Channell), xuan2005@ufl.edu (C. Xuan).

0012-821X/$ – see front matter © 2009 Elsevier B.V. All rights reserved.
doi:10.1016/j.epsl.2009.04.020

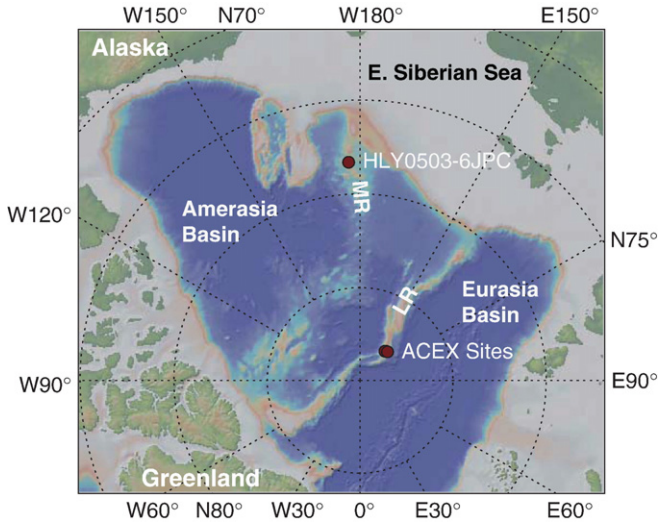

Fig. 1. Location of Core HLY0503-6JPC and the IODP Expedition 302 (ACEX) sites. LR denotes Lomonosov Ridge, MR denotes Mendeleev Ridge.

In the last 20 years, the revelation of numerous polarity excursions within the Brunhes and Matuyama Chrons has been one of the most important developments in paleomagnetism. Following Champion et al. (1988), who made the case for 8 excursions within the Brunhes Chron, the number of excursions in the Brunhes Chron has proliferated to 12–15 although only about seven Brunhes-aged excursions have been adequately documented and age calibrated (Lund et al., 2006; Laj and Channell, 2007). The recording of magnetic excursions is uncommon because their brief duration restricts them to sedimentary sequences characterized by high fidelity magnetic recording and sedimentation rates in excess of ~10 cm/kyr (Roberts and Winklhofer, 2004). In the Arctic Ocean and Norwegian–Greenland Sea, cores with mean sedimentation rates that are an order of magnitude lower have apparently recorded numerous excursions. For example, the ACEX mean sedimentation rate for the Brunhes Chron is estimated to be 1.8 cm/kyr (O'Regan et al., 2008) with a Brunhes Chronozone thickness of 14.3 m. Outside the Arctic and Norwegian–Greenland Sea, the thickness of the Brunhes Chronozone exceeds 80 m in sections where Brunhes excursions have been observed. The better estimates of excursion duration from the North Atlantic lie in the few (1–3) thousand-year range (e.g. Laj et al., 2000; Lund et al., 2005; Channell, 2006). Sediment cores from the Arctic Ocean and Norwegian–Greenland Sea usually yield longer duration estimates for geomagnetic excursions. For example, assuming the labeling of excursions in the Arctic region is correct and adopting excursion ages determined outside the region, the Mono Lake, Laschamp and Blake excursions have apparent durations of 15, 20 and 26 kyr, respectively, in Yermak Core PS2212 (Nowaczyk et al., 1994). A related anomaly common to these high latitude cores is that the cumulative percentage thickness of

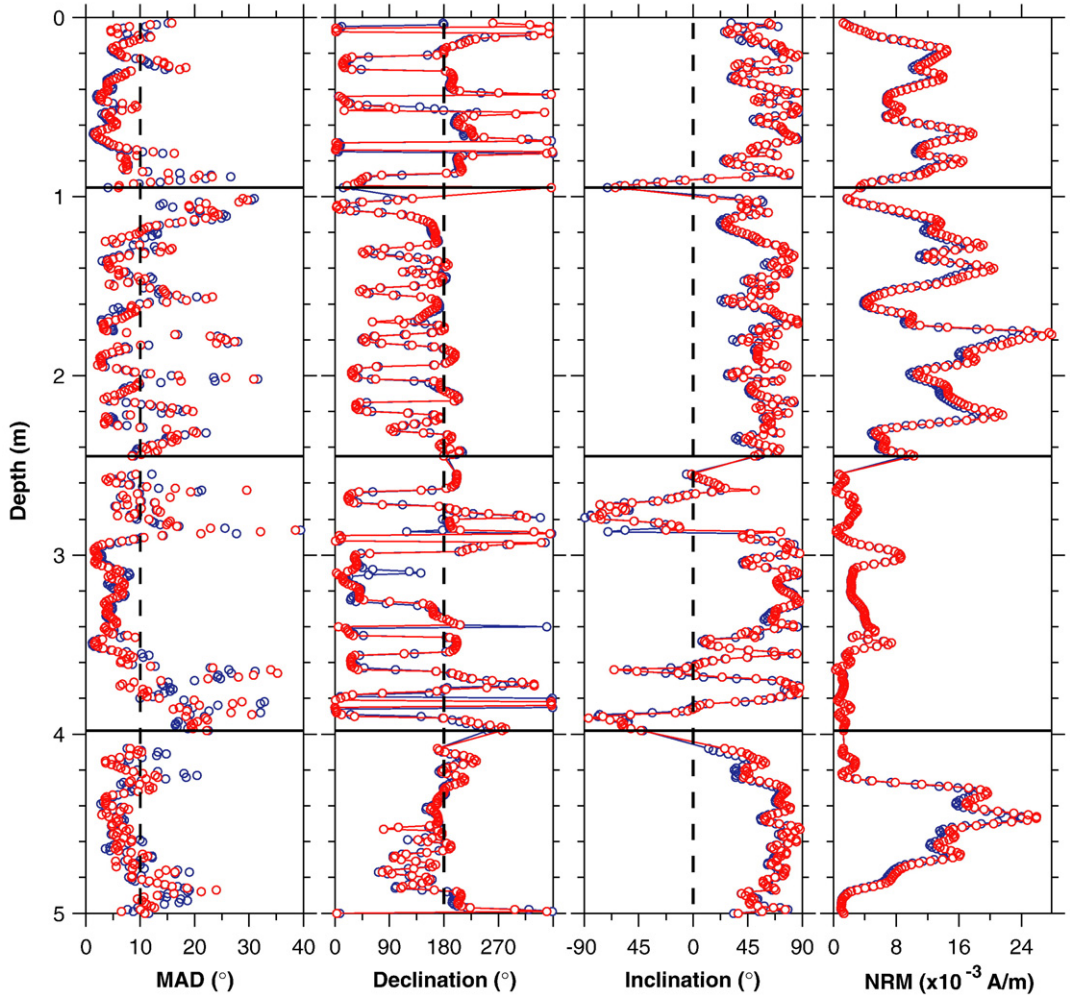

Fig. 2. Core HLY0503-6JPC: Component declination and inclination with maximum angular deviation (MAD) statistic calculated for the 20–80 mT peak alternating field range using two demagnetization sequences for the three sample axes: *XYZ* (blue) and *ZXY* (red). NRM intensity is shown after demagnetization at peak fields of 10 mT for the *XYZ* sequence (blue) and *ZXY* sequence (red). Note that declination values are arbitrary as core was not oriented in azimuth. Section breaks are indicated. (For interpretation of the references to colour in this figure legend, the reader is referred to the web version of this article.)

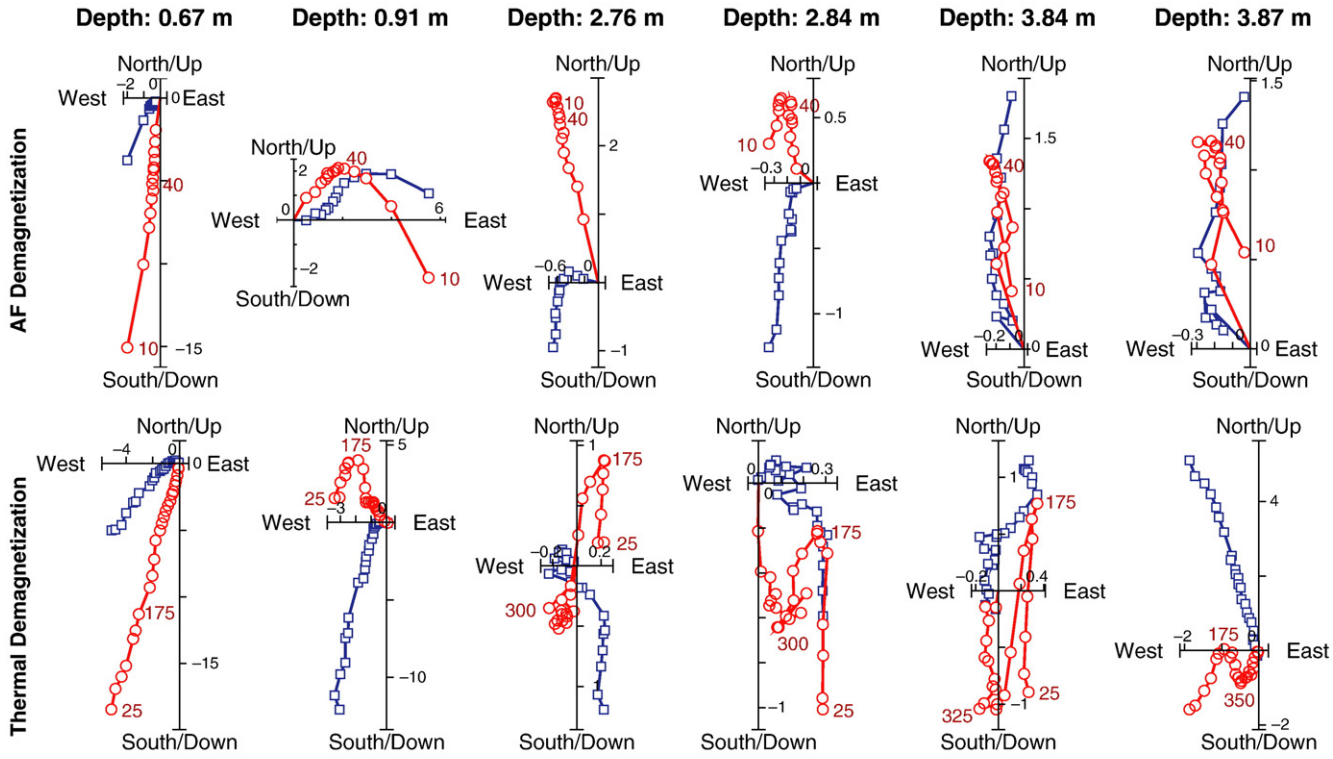

Fig. 3. Orthogonal projection of AF demagnetization (above) and thermal demagnetization (below). Peak demagnetizing field ranges are 10–60 mT in 5 mT steps then 60–100 mT in 10 mT steps. Temperature ranges are 25–600 °C in 25 °C steps. Circles (red) and squares (blue) denote projection on vertical and horizontal planes, respectively. Declination values are arbitrary as core was not oriented in azimuth. Unit for intensity scale is mA/m. Meter levels correspond to meter levels in Fig. 2. (For interpretation of the references to colour in this figure legend, the reader is referred to the web version of this article.)

zones of negative inclination is far greater than expected. For example, zones of negative inclination occupy ~50% of the recovered sedimentary sequence in Fram Strait Core PS1535 (Nowaczyk and Baumann, 1992; Nowaczyk and Frederichs, 1999) and >50% for the top 4 m of the section interpreted to represent the last 120 kyr in Core PS2212 from the Yermak Plateau (Nowaczyk et al., 1994). Fortuitous fluctuations in sedimentation rates have to be invoked to explain these "amplified" excursion records.

2. Magnetic properties of Core HLY0503-6JPC

The natural remanent magnetization (NRM) of one of the cores (Core HLY0503-6JPC at 78° 17.6′N and 176° 59.2′W) taken from the Mendeleev Ridge (Fig. 1) during the Healy–Oden Trans-Arctic Expedition 2005 (HOTRAX) expedition is characterized by negative component inclinations within the uppermost few meters of the core (Fig. 2). The

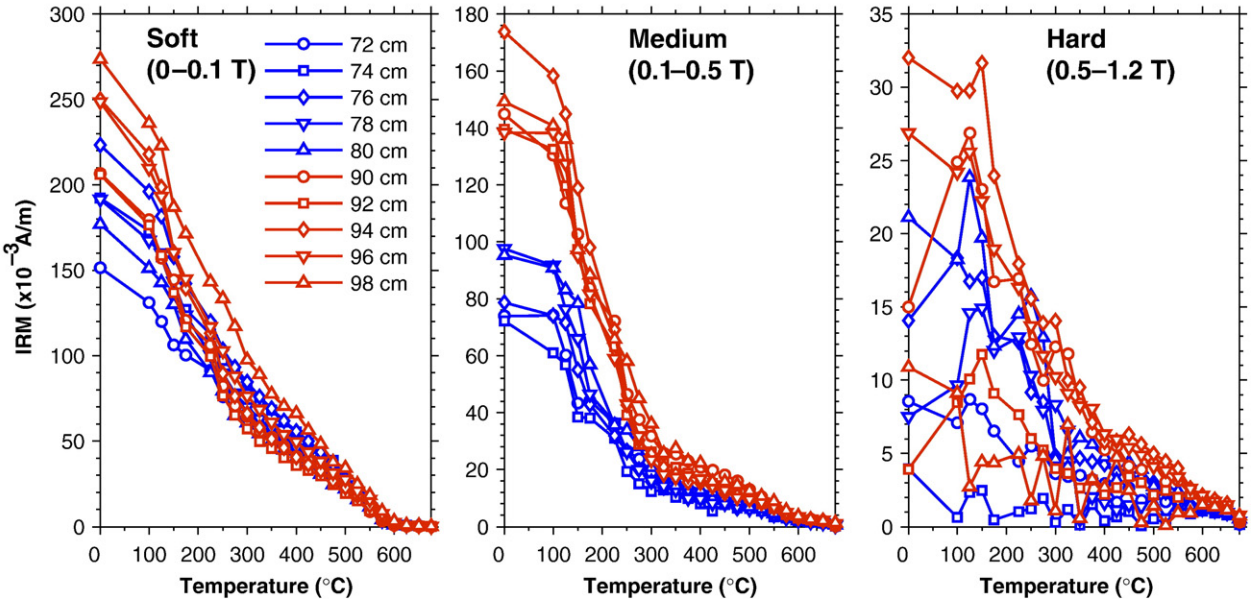

Fig. 4. Thermal demagnetization of three-axis isothermal remanent magnetizations (IRM) imposed orthogonally and sequentially in DC fields of 1.2 T (hard), 0.5 T (medium) and 0.1 T (soft), for samples collected from intervals showing positive (blue) and negative (red) component inclinations. Refer to Fig. 2 for positions of the samples. (For interpretation of the references to colour in this figure legend, the reader is referred to the web version of this article.)

sediments comprise brown to yellow-gray silts and silty–clays with occasional sandy layers. The chronology of sedimentation on the Mendeleev Ridge is based on amino acid racemization with accompanying radiocarbon ages, and sparse biostratigraphic data. The mid-Brunhes Chron at 300 ka is estimated to lie at ~5 m depth in Core HLY0503-6JPC and other HOTRAX cores collected from the Mendeleev Ridge (Polyak et al., 2004; Kaufman et al., 2008), consistent with few-cm/kyr scale sedimentation rates (Backman et al., 2004). The important point for the purposes of this paper is that the entire 5 m represented in Fig. 2 constitutes sediment deposited during the Brunhes Chron.

The NRM data were partly acquired from u-channel ($2\times2\times150$ cm^3) samples. The NRM of each u-channel was measured at 1 cm intervals before demagnetization and after alternating field (AF) demagnetization at 14 steps in the 10–100 mT peak field range. For each step, the samples were measured after two demagnetization sequences for the *X*, *Y* and *Z* sample axes. The first *XYZ* demagnetization sequence was followed by measurement, and then the *ZXY* demagnetization sequence was followed by repeat measurement at the same demagnetization step. The purpose of the procedure was to monitor any spurious anhysteretic remanence (ARM) acquisition during AF demagnetization. AF-derived NRM component magnetization directions include several intervals of negative component inclination, with inclinations generally lower than the expected inclination (84°) for a geocentric axial dipole field at the site (Fig. 2). The component magnetization directions, isolated in the 20–80 mT peak field range using the standard procedure (Kirschvink, 1980), are reasonably well-defined (Fig. 3) as indicated by maximum angular deviation (MAD) values often less than 10° (Fig. 2). Choosing a different demagnetization range, other than 20–80 mT, would not appreciably change the result, and by using a uniform demagnetization range, the MAD values serve to indicate the variation in definition of the component direction. Note that the directions are not dependent on the demagnetization sequence (*XYZ* or *ZXY*), ruling out appreciable influence from spurious magnetizations acquired during the AF demagnetization process (Fig. 2).

Ten discrete samples (approximately $2\times2\times2$ cm^3) were collected from both positive and negative inclination intervals of the u-channel used for AF demagnetization experiments (Fig. 2). Isothermal remanent magnetizations (IRM) acquired in DC fields of 1.2 T, 0.5 T, and 0.1 T were imposed along three orthogonal axes of the discrete samples (method of Lowrie, 1990). Thermal demagnetization of each orthogonal component indicates that the samples are dominated by soft and medium-coercivity IRM components (Fig. 4). The low- and medium-coercivity IRMs, acquired in 0.1 T and 0.5 T fields, respectively, have a maximum blocking temperatures (580 °C) indicative of magnetite. An abrupt drop in intensity for the medium-coercivity fraction below 300 °C (Fig. 4) is interpreted to indicate the presence of (titano)maghemite, that loses its remanence due to inversion at temperatures above 250 °C (Readman and O'Reilly, 1970, 1972; Özdemir, 1987). An alternative explanation, the presence of magnetic iron sulfides, can be discarded based on the oxidized nature of these red-brown sediments, the lack of evidence for iron sulfides from X-ray diffraction, scanning electron microscopy (SEM), and gas chromatography for the detection of sedimentary sulfur performed at Old Dominion University by C. Lingle and D. Darby using the very sensitive methods described by Cutter and Oatts (1987). Samples from intervals characterized by negative NRM inclination components (red in Fig. 4) have a higher proportion of the medium-coercivity (titanomaghemite) magnetic component.

Magnetic moment in a 0.5 T field was measured as a function of temperature, in helium atmosphere, on a vibrating sample magnetometer (Fig. 5A) and during thermal cycling (Fig. 5B). The decrease in moment below 300 °C and below 580 °C (Fig. 5A) can be associated with the presence of titanomaghemite and magnetite, respectively. The increase in magnetic moment on cooling from temperatures above 400 °C (Fig. 5B) is associated with inversion of titanomaghemites to intergrowths of Ti-poor spinel (magnetite) with a Ti-rich rhombohedral phase near ilmenite (Readman and O'Reilly, 1970, 1972; Özdemir and Banerjee, 1984; Özdemir, 1987; Krasa and Matzka, 2007; Soubrand-Colin et al., 2009). The inversion of titanomaghemite to a more magnetic (magnetite) phase in this temperature range is more likely than the possibility of a restricted titanium content in titanomagnetite as the cause for the observed decrease in magnetization at ~300 ° C (Figs. 4 and 5).

On monitoring of magnetization at low temperatures (Fig. 6), evidence for a suppressed Verwey transition at ~120 K, in samples from both positive and negative inclination intervals, is consistent with the presence of magnetite and maghemite. The maghematization of magnetite suppresses the Verwey transition relative to its appearance in the unoxidized magnetite, and the transition is likely to be smeared over a wider range of temperatures (say 70–120 K) than for stiochiometric magnetite (Özdemir et al., 1993).

Thermal demagnetization of the NRM was carried out on discrete (8 cm^3) samples, collected alongside the u-channel samples in plastic cubes. The NRM was measured without demagnetization, and then

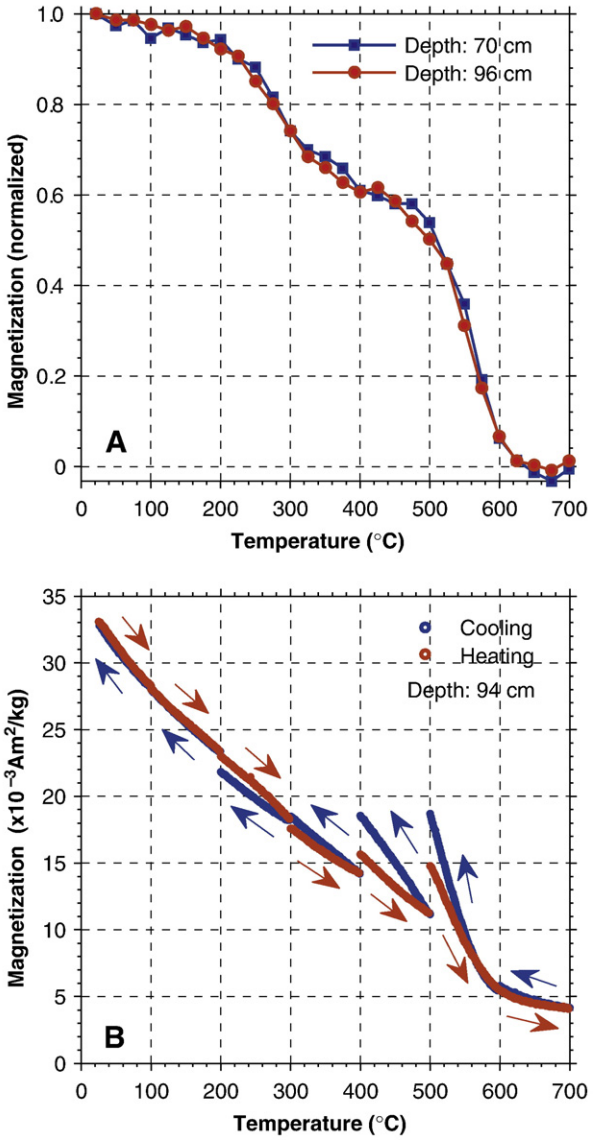

Fig. 5. (A) Magnetization in a 0.5 T applied field derived from hysteresis loops measured at increasing temperatures (in 25 °C steps in an helium atmosphere) using a vibrating sample magnetometer (VSM). Values have been normalized to the room temperature measurement. (B) Magnetization in a 0.5 T applied field measured during thermal cycling where red and blue lines denote heating and cooling, respectively. The sample was heated in 100 °C increments during measurement at ~1 °C steps, then cooled by 100 °C during further measurement, then heated through 100 °C without measurement to the onset temperature of the next heating cycle. Refer to Fig. 2 for positions of samples. (For interpretation of the references to colour in this figure legend, the reader is referred to the web version of this article.)

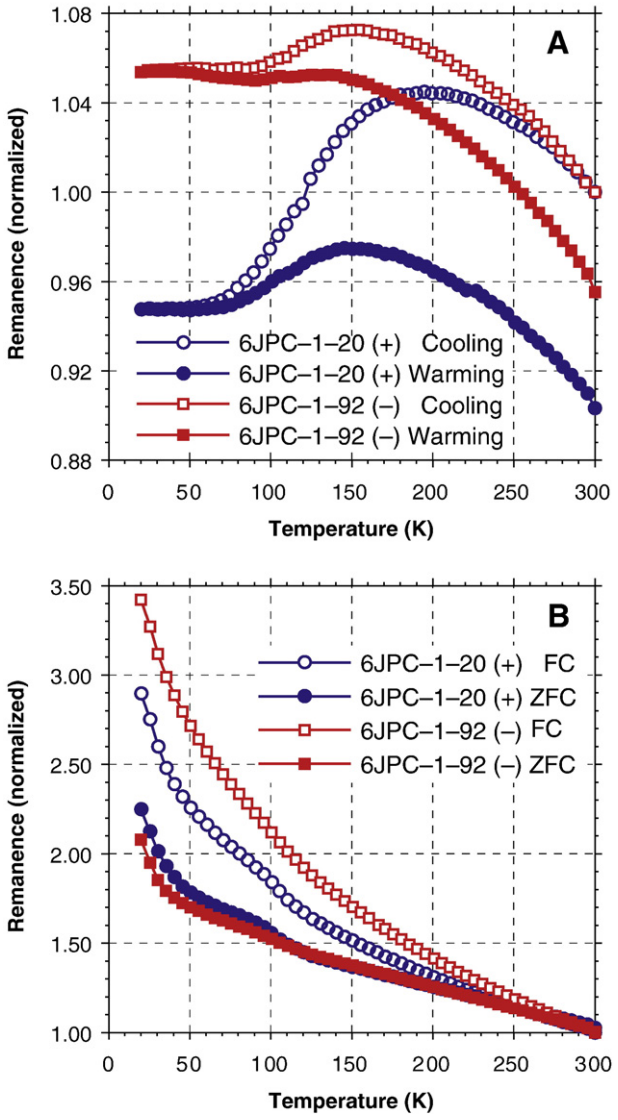

Fig. 6. (A) Saturation remanent magnetization (SIRM), acquired in a 2.5 T field at room temperature, on cooling and warming; measured using a magnetic properties measurement system (MPMS). Measurements have been normalized to the room temperature magnetization of the sample on cooling. (B) Field cooled (2.5 T), and zero-field cooled, low-temperature SIRM measured on warming. Measurements have been normalized to the field cooled magnetization of the sample at room temperature. Blue and red curves denote samples from positive and negative inclination intervals, respectively (see Fig. 2). (For interpretation of the references to colour in this figure legend, the reader is referred to the web version of this article.)

the samples were dried in a stream of helium gas prior to extraction from the plastic containers, and wrapping in Al foil for thermal treatment. Magnetization directions were found to be consistent before and after drying and wrapping. Thermal demagnetization revealed NRM components with negative inclination that have blocking temperatures largely, but not entirely, below 300 °C (Fig. 3). This negative inclination component is superimposed on a higher blocking temperature component with maximum blocking temperatures up to 600 °C that usually has positive inclination and may represent the direction of the geomagnetic field close to the time of sediment deposition. For one sample shown in Fig. 3 (at 0.91 m), the negative inclination component appears to have blocking temperatures up to 500 °C. These observations implies that the negative inclination components resolved by AF demagnetization (Figs. 2 and 3) are carried by the mineral (titanomaghemite) that has blocking temperatures largely below 300 °C.

As the sediment was deposited in the Brunhes Chron, the negative inclination component, apparently carried by titanomaghemite, may have been generated by partial self-reversal. The thermo-magnetic experiments (Figs. 4 and 5) indicate that the presence of titanomaghemite is not restricted to zones characterized by negative inclinations (Fig. 2). Note that the zones of negative inclination correspond to intervals of low NRM intensity (Fig. 2), implying the presence of anti-parallel magnetization components in these intervals. In summary, zones with negative component inclination as revealed by AF demagnetization generally show, on thermal demagnetization, positive inclination components with higher blocking temperatures superimposed on negative inclination components with lower blocking temperatures. The coercivity spectra of titanomagnetite and titanomaghemite overlap, but blocking temperature spectra of the two phases are distinct.

3. XRD and SEM observations

Magnetic extracts were made by dispersing a small amount of sediment (~30 g) in a sodium metaphosphate solution, and using a magnetic finger (comprising a string of rare earth magnets in a glass test tube) to repeatedly separate magnetic particles. Centrifuging with a heavy liquid (sodium polytungstate with density 2.84 g/cc) was used to refine the extract. Extracts were washed using water, then methanol, and dried for scanning electron microscopy (SEM) using a Zeiss EVO microscope and EDAX (Genesis) energy dispersive analysis. Images and EDAX analyses indicate the presence of micron-sized titanomagnetite/titanomaghemite grains with varying amounts of titanium and compositions in the $x = 0.35$–0.65 range, with ancillary quartz and sphene (Fig. 7). The larger Fe–Ti rich particle in Fig. 7 shows indications of compositional zoning.

X-ray diffraction (XRD) for unheated magnetic separate, and magnetic separate heated to 700 °C, indicate peaks, calibrated using a silica standard, corresponding to magnetite/maghemite and quartz (Fig. 8). The XRD peak at $2\theta = 35.63°$ for the unheated separate lies close to the peak for (titano)maghemite derived from the [113] diffraction plane. The 2θ value (35.63°) is larger than the 2θ value for magnetite standards (35.42°), and the peak is shifted to lower values of 2θ (by ~0.3°) after heating the separate, consistent with (titano) maghemite in the unheated sample being inverted to magnetite in the heated sample. The diffraction peaks close to $2\theta = 57.0°$–$57.5°$ and 62.5°–63.5° (Fig. 8) are derived from the [115] and [440] diffraction planes of magnetite/maghemite, respectively. Based on comparison with standards for magnetite (where $2\theta = 56.943°$ and 62.515°) and maghemite (where $2\theta = 57.271°$ and 62.925°), the peaks are consistent with mixtures of titanomaghemite and titanomagnetite. Both peaks are shifted to lower values of 2θ on heating (again by about 0.3°) consistent with the inversion of (titano)maghemite to low-Ti magnetite (Fig. 8).

The asymmetric shape of the three diffraction peaks A, B and C (Fig. 8) is interpreted to indicate the co-existence of (titano) maghemite and (titano)magnetite in both the unheated and heated samples. We attempt to model the diffraction peaks, using pseudo-Voigt functions, to derive two components which best fit each of the three diffraction peaks (Table 1). For the unheated extract, the average lattice parameters for the two modeled components (8.3388 Å and 8.3773 Å) indicate high oxidation states with $z > 0.9$ (Readman and O'Reilly, 1972). For the heated extract, higher average lattice parameters (8.3781 Å and 8.4230 Å) indicate lower oxidation states ($z = 0.7$ for $x = 0.6$), interpreted to be due to partial inversion of titanomaghemite to Ti-poor magnetite on heating.

4. Self-reversal in titanomaghemite

Individual single-domain titanomagnetite grains carrying thermal remanent magnetization (TRM) can be statistically aligned in the

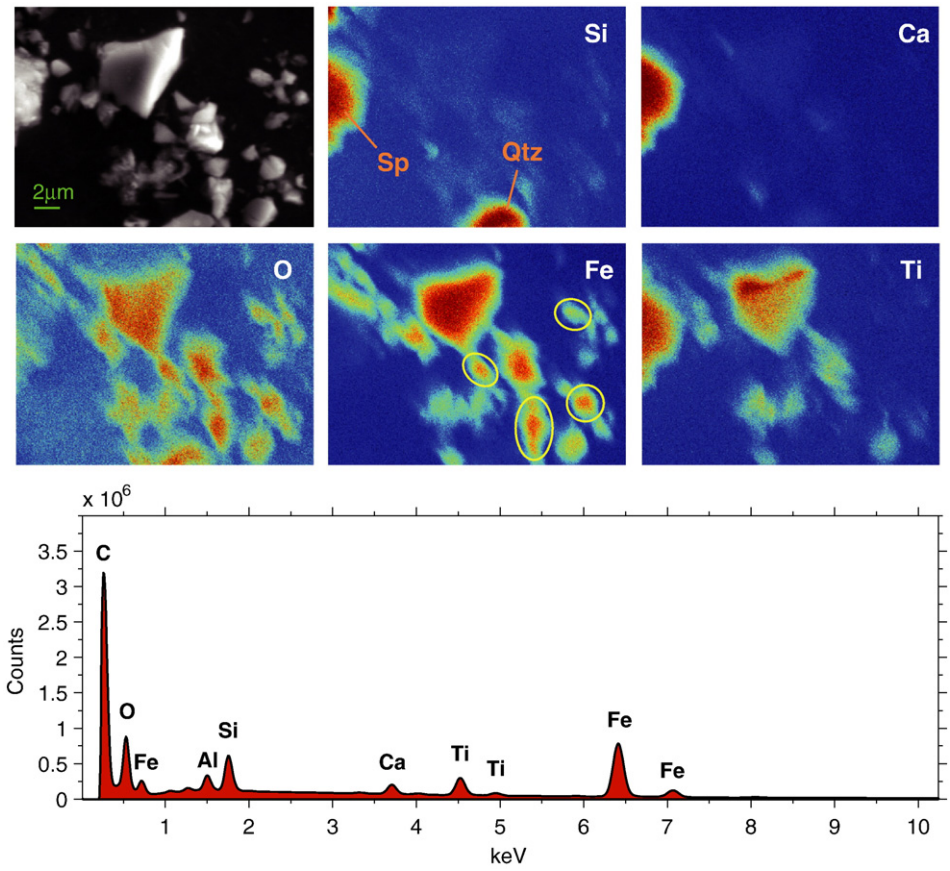

Fig. 7. Energy dispersive (EDAX) elemental mapping of micron-sized grains from an unheated magnetic extract. The grains in the image comprise titanomagnetite/titanomaghemite, Ti-poor magnetite/maghemite (circled), sphene/titanite (Sp) and quartz (Qtz). The total X-ray spectrum acquired during the mapping is also displayed, where carbon (C) and aluminum (Al) are attributed to background noise from the carbon tape and aluminum stub.

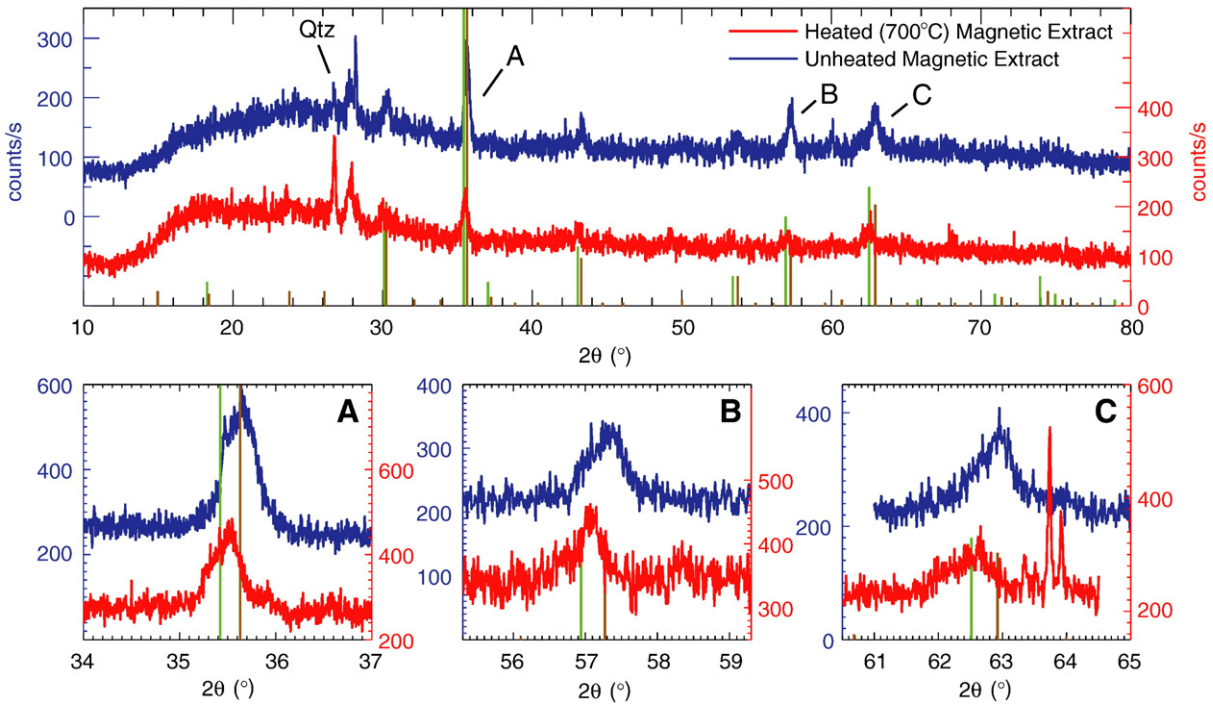

Fig. 8. X-ray diffraction (XRD) results for unheated magnetic extract (blue) and heated (to 700 °C) magnetic extract (red), with higher resolution scans around the three peaks (A, B, C) associated with titanomaghemite and titanomagnetite. The positions and magnitudes of XRD peaks for magnetite (green) and maghemite (orange) standards are indicated. Ancillary peaks are associated with quartz (Qtz). Diffraction peaks close to $2\theta = 35.7°, 57.4°$ and $62.9°$ are interpreted as composite peaks due to mixtures of (titano)maghemite and (titano)magnetite. The displacement of the peaks to lower values of 2θ on heating is interpreted as being due to partial inversion of titanomaghemite to Ti-poor magnetite. (For interpretation of the references to colour in this figure legend, the reader is referred to the web version of this article.)

Table 1
2θ values and estimated lattice parameters (L.P.) for Component 1 and Component 2 derived by modeling the three asymmetric X-ray diffraction peaks (Fig. 8).

Samples	Components	Diffraction plane						Average L.P. (Å)
		[113]		[115]		[440]		
		2θ (°)	L.P. (Å)	2θ (°)	L.P. (Å)	2θ (°)	L.P. (Å)	
Heated (700 °C) magnetic extract	Component 1	35.3124	8.4230	56.7404	8.4230	62.4455	8.4060	8.4173
	Component 2	35.5130	8.3768	57.0652	8.3793	62.6478	8.3818	8.3793
Unheated magnetic extract	Component 1	35.5050	8.3787	57.1686	8.3652	62.5946	8.3879	8.3773
	Component 2	35.6909	8.3367	57.4112	8.3331	62.9357	8.3467	8.3388

ambient field during or shortly after sediment deposition to yield a detrital remanent magnetization (DRM). Seafloor oxidation of the titanomagnetite grains results in the TRM of individual grains being partially or completely transformed to a chemical remanent magnetization (CRM) carried by titanomaghemite. The oxidation of titanomagnetite to titanomaghemite on the seafloor is restricted to sedimentary environments characterized by low accumulation rates, such as the red-clay facies of the central North Pacific (Kent and Lowrie, 1974; Johnson et al., 1975), where slow burial enables oxidation at the sediment–water interface. The CRM of the titanomaghemite is usually considered, based on experimental data, to parallel the original TRM of the titanomagnetite grain (Johnson and Merrill, 1974; Özdemir and Dunlop, 1985), however, the oxidized phase can become magnetized anti-parallel to the host phase due either to a change in the balance of anti-parallel moments in the ferrimagnetic sublattices of the spinel structure during oxidation, or alternatively by negative magnetostatic interactions between magnetic phases.

Titanohematites and titanomaghemites have been central to models of the self-reversal phenomena since the 1950s. The best documented model of self-reversal involves high temperature exsolution of phases of titanohematite with bulk composition near $y = 0.5$. Titanohematites with this bulk composition are rare but include the famous Haruna dacite (Nagata et al., 1952; Uyeda, 1958) and more recently investigated examples (e.g. Bina et al., 1999). Models of self-reversal involving titanomaghemite can be traced to the "ionic ordering" models of Verhoogen (1956, 1962) in which highly oxidized titanomaghemites (with high values of x and z) lead to partial self-reversal of chemical remanence (CRM) relative to the remanence direction in the host titanomagnetite (O'Reilly and Banerjee, 1966; Schult, 1968, 1971; Ozima and Sakamoto, 1971; Readman and O'Reilly, 1970, 1972). The process of low-temperature oxidation of titanomagnetite to titanomaghemite can be accomplished by diffusion of Fe^{2+} ions from the B (octahedral) sublattices beginning at the surface of the grain (O'Reilly, 1984; Dunlop and Özdemir, 1997). The inverse spinel structure is unchanged during oxidation but vacancies develop at the octahedral (B sublattice) sites of leached Fe^{2+} ions. The leached Fe^{2+} ions are converted to Fe^{3+}, and may be exchange coupled at the surface of the grain. During high degrees of low-temperature oxidation, ferrimagnetic titanomagnetite with a magnet
ically dominant B (octahedral) sublattice can be transformed to a titanomaghemite with a dominant A (tetrahedral) sublattice moment, aligned anti-parallel to the B sublattice moment. This change is accompanied by a decrease in the Fe/Ti ratio.

In mid-ocean ridge basalts, Doubrovine and Tarduno (2004) associated self-reversed NRM components, with blocking temperatures below 325 °C, to titanomaghemite formed by low-temperature seafloor oxidation. In the case of the Arctic sediments studied here, a detrital remanent magnetization (DRM) carried by single-domain titanomagnetite appears to have been converted by sea floor oxidation to a titanomaghemite carrying a partially self-reversed CRM. The apparent stratigraphic correlation of intervals of negative inclination within the Arctic Ocean (e.g. Spielhagen et al., 2004; O'Regan et al., 2008) implies that the alteration of detrital titanomagnetite to titanomaghemite is lithologically controlled. Organic carbon records from the Arctic Ocean and Norwegian–Greenland Sea indicate the dominance of terrigenous organic matter, presumably because sea-ice coverage inhibited marine productivity (Ikehara et al., 1999; Stein et al., 2003; Expedition 303 Scientists, 2006). The refractory nature of the (terrigenous) organic matter in the Arctic region results in the low activity of (sulfate) reducing microbes, thereby maintaining oxidizing diagenetic conditions.

5. Conclusions

In Core HLY0503-6JPC from the Mendeleev Ridge, the evidence for self-reversal lies in the identification of an authigenic carrier of NRM (titanomaghemite) and the observation that this mineral carries an NRM component, isolated by thermal demagnetization, that is approximately anti-parallel to the NRM of primary titanomagnetite. AF demagnetization does not reveal this same anti-parallelism (Fig. 3), presumably due to overlapping coercivity spectra of the two remanence carriers. AF demagnetization generally implies a primary magnetization component carrying positive and negative inclinations that mimic polarity zones or excursions (Fig. 2).

The presence of titanomaghemite with negative inclinations in this core may be relevant to the long-standing problem of interpreting magnetostratigraphies from the Arctic Ocean and Norwegian–Greenland Sea. Up to now, AF demagnetization has been used exclusively in magnetic studies of marine sediments from the Arctic Ocean and Norwegian–Greenland Sea. Due to the similar coercivities of titanomagnetite and titanomaghemite, AF demagnetization of these Arctic sediments does not reveal that positive and negative inclination components are carried by different mineral phases. As the global record of geomagnetic excursions has improved, the propensity for, and duration of, excursions in the Arctic Ocean and Norwegian–Greenland Sea has become increasingly anomalous, and requires special characteristics of the geomagnetic field at high latitudes for which there is little evidence in the modern field or in numerical models of field behavior. For this reason, the evidence for partial self-reversed CRM in Arctic sediments from the Mendeleev Ridge has implications for Arctic sediments in general, and for diagenetic alteration of titanomagnetite DRM in oxidizing conditions.

Acknowledgements

We thank L. Polyak for facilitating the core sampling at Ohio State University. Ian Snowball, Mark Dekkers and an anonymous reviewer provided valuable comments on an early version of this manuscript. Dennis Darby and Carie Lingle provided useful information on sediment chemistry. Junghun Jang and Ann Heatherington assisted with XRD and SEM analyses, respectively. The Institute of Rock Magnetism (IRM) in Minnesota provided a visiting fellowship, and assistance in data acquisition. The IRM is supported by the Keck Foundation, the National Science Foundation, and the University of Minnesota. Research was supported by the US National Science Foundation through award ARC-0806309.

References

Backman, J., Jakobsson, M., Løvlie, R., Polyak, L., Febo, L.A., 2004. Is the central Arctic Ocean a sediment starved basin? Quat. Sci. Rev. 23, 1435–1454.

Backman, J., Moran, K., McInroy, D.B., Mayer, L.A., Expedition 302 Scientists, 2006. Proc. IODP. Integrated Ocean Drilling Program Management International, Inc., Edinburgh, p. 302. 10.2204/iodp.proc.302.2006.

Backman, J., Jakobsson, M., Frank, M., Sangiorgi, F., Brinkhuis, H., Stickley, C., O'Regan, M., Løvlie, R., Pälike, H., Spofforth, D., Gattacecca, J., Moran, K., King, J., Heil, C., 2008. Age model and core-seismic integration for the Cenozoic Arctic Coring Expedition sediments from the Lomonosov Ridge. Palaeoceanography 23, PA1S03. doi:10.1029/2007PA001476.

Bina, M., Tanguy, J.C., Hoffman, V., Prévot, M., Listanco, E.L., Keller, R., Fedr, K.T.h., Goguitchaichvili, A.T., Punongbayan, R.S., 1999. A detailed magnetic and mineralogical study of self-reversed dacitic pumices from the 1991 Pinatubo eruption (Philippines). Geophys. J. Int. 138, 159–178.

Bleil, U., Gard, G., 1989. Chronology and correlation of Quaternary magnetostratigraphy and nannofossil biostratigraphy in Norwegian–Greenland Sea sediments. Geol. Rundschau 78, 1173–1187.

Champion, D.E., Lanphere, M.A., Kuntz, M.A., 1988. Evidence for a new geomagnetic reversal from lava flows in Idaho: discussion of short polarity reversals in the Brunhes and late Matuyama Chrons. J. Geophys. Res. 93, 11667–11680.

Channell, J.E.T., 2006. Late Brunhes polarity excursions (Mono Lake, Laschamp, Iceland Basin and Pringle Falls) recorded at ODP Site 919 (Irminger Basin). Earth Planet. Sci. Lett. 244, 378–393.

Clark, D.L., 1970. Magnetic reversals and sedimentation rates in the Arctic Basin. Geol. Soc. Amer. Bull. 81, 3129–3134.

Cronin, T., Smith, S.A., Eynaud, F., O'Regan, M., King, J., 2008. Quaternary paleoceanography of the central Arctic based on Integrated Ocean Drilling Program Arctic Coring Expedition 302 foraminiferal assemblages. Palaeoceanography 23, PA1Si8. doi:10.1029/2007PA001484.

Cutter, G.A., Oatts, T.J., 1987. Determination of dissolved sulfide and sedimentary sulfur speciation using gas chromatography-photionization detection. Anal. Chem. 59, 717–721.

Doubrovine, P.V., Tarduno, J.A., 2004. Self-reversed magnetization carried by titanomaghemite in oceanic basalts. Earth Planet. Sci. Lett. 222, 959–969.

Dunlop, D.J., Özdemir, O., 1997. Rock Magnetism: Fundamentals and Frontiers. Cambridge University Press. 573pp.

Expedition 302 Scientists, Sites M0001-M0004 (2006), In: Backman, J., Moran, K., McInroy, D.B., Mayer, L.A.,and Expedition 302 Scientists, Proceedings of the Integrated Ocean Drilling Program, 302, 1–169.

Ikehara, M., Kawamura, K., Ohkouchi, N., Taira, A., 1999. In: Jansen, E., Raymo, M.E., Blum, P., Herbert, T. (Eds.), Organic Geochemistry of Greenish Clay and Organic-Rich Sediments Since the Early Miocene from Hole 985A, Norway Basin. Proc. ODP, Sci. Results, vol. 162. Ocean Drilling Program, College Station, TX, pp. 209–216.

Johnson, H.P., Merrill, R.T., 1974. Low-temperature oxidation of single domain magnetite. J. Geophys. Res. 79, 5533–5534.

Johnson, H.P., Lowrie, W., Kent, D.V., 1975. Stability of anhysteretic remanent magnetization in fine and coarse magnetite and maghemite particles. Geophys. J. R. Astron. Soc. 41, 1–10.

Kent, D.V., Lowrie, W., 1974. Origin of magnetic instability in sediment cores from the central North Pacific. J. Geophys. Res. 79, 2987–3000.

Krasa, D., Matzka, J., 2007. Inversion of titanomaghemite in oceanic basalt during heating. Phys. Earth Planet. Inter. 160, 169–179.

Kaufman, D.S., Polyak, L., Adler, R., Channell, J.E.T., Xuan, C., 2008. Dating late Quaternary planktonic foraminifer Neogloboquadrina pachyderma from the Arctic Ocean by using amino acid racemization. Paleoceanography 23, PA3224.

Kirschvink, J.L., 1980. The least squares lines and plane analysis of paleomagnetic data. Geophys. J.R. Astr. Soc. 62, 699–718.

Laj, C., Kissel, C., Mazaud, A., Channell, J.E.T., Beer, J., 2000. North Atlantic PaleoIntensity Stack since 75 ka (NAPIS-75) and the duration of the Laschamp event. Phil. Trans. R. Soc. Series A. 358, 1009–1025.

Laj, C., Channell, J.E.T., 2007. Geomagnetic excursions. In: Kono, M. (Ed.), Treatise on Geophysics. . Geomagnetism, vol. 5. Elsevier, Amsterdam, pp. 373–416. Chapter 10.

Løvlie, R., Markussen, B., Sejrup, H.P., Thiede, J., 1986. Magnetostratigraphy in three Arctic Ocean sediment cores; arguments for magnetic excursions within oxygen-isotope stage 2–3. Phys. Earth Planet. Inter. 43, 173–184.

Lowrie, W., 1990. Identification of ferromagnetic minerals in a rock by coercivity and unblocking temperature properties. Geophys. Res. Lett. 17, 159–162.

Lund, S.P., Schwartz, M., Keigwin, L., Johnson, T., 2005. Deep-sea sediment records of the Laschamp geomagnetic field excursion (~41,000 calendar years before present). J. Geophys. Res. 110, B04101. doi:10.1029/2003JB002943.

Lund, S.P., Stoner, J.S., Channell, J.E.T., Acton, G., 2006. A summary of Brunhes paleomagnetic field variability recorded in Ocean Drilling Program cores. Phys. Earth Planet. Inter. 156, 194–204.

Markussen, B., Zahn, R., Thiede, J., 1985. Late Quaternary sedimentation in the eastern Arctic Basin: stratigraphy and depositional environment. Palaeogeogr., Palaeoclimatol. Palaeoecol. 50, 271–284.

Nagata, T., Uyeda, S., Akimoto, S., 1952. Self-reversal of thermoremanent magnetization of igneous rocks. J. Geomagn. Geoelectr. 4, 22–38.

Nowaczyk, N.R., Baumann, M., 1992. Combined high-resolution magnetostratigraphy and nannofossil biostratigraphy for late Quaternary Artic Ocean sediments. Deep Sea Res. 39, 567–601.

Nowaczyk, N.R., Antonow, M., 1997. High resolution magnetostratigraphy of four sediment cores from the Greenland Sea — I. Identification of the Mono Lake excursion, Laschamp and Biwa I/Jamaica geomagnetic polarity events. Geophys. J. Int. 131, 310–324.

Nowaczyk, N.R., Frederichs, T.W., 1999. Geomagnetic events and relative paleointensity variations during the last 300 ka as recorded in Kolbeinsey Ridge Sediments, Iceland Basin — indication for a strongly variable geomagnetic field. Int. J. Earth Sci. 88, 116–131.

Nowaczyk, N.R., Knies, J., 2000. Magnetostratigraphic results from the eastern Arctic ocean: AMS 14C ages and relative paleointensity data of the Mono Lake and Laschamp geomagnetic reversal excursions. Geophys. J. Int. 140, 185–197.

Nowaczyk, N.R., Frederichs, T.W., Eisenhauer, A., Gard, G., 1994. Magnetostratigraphic data from late Quaternary sediments from the Yermak Plateau, Arctic Ocean: evidence for four geomagnetic polarity events within the last 170 Ka of the Brunhes Chron. Geophys. J. Int. 117, 453–471.

O'Regan, M., King, J., Backman, J., Jakobsson, M., Palike, H., Moran, K., Heil, C., Sakamoto, T., Cronin, T.M., Jordan, R.W., 2008. Constraints on the Pleistocene chronology of sediments from the Lomonosov Ridge. Paleoceanography 23, PA1S19. doi:10.1029/2007PA001551.

O'Reilly, W., 1984. Rock and Mineral Magnetism. Blackie & Sons Ltd., Glasgow. 220 pp.

O'Reilly, W., Banerjee, S.K., 1966. Oxidation of titanomagnetites and self-reversal. Nature 211, 26–28.

Özdemir, O., 1987. Inversion of titanomaghemites. Phys. Earth Planet. Inter. 46, 184–196.

Özdemir, O., Banerjee, S.K., 1984. High temperature stability of maghemite (g-Fe2O3). Geophys. Res. Lett. 11, 161–164.

Özdemir, O., Dunlop, D.J., 1985. An experimental study of Chemical Remanent Magnetizations of synthetic monodomain titanomaghemites with initial thermoremanent magnetizations. J. Geophys. Res. 90, 11,513–11,523.

Özdemir, O., Dunlop, D.J., Moskowitz, B., 1993. The effect of oxidation on the Verwey transition in magnetite. Geophys. Res. Lett. 20 (16), 1671–1674.

Ozima, M., Sakamoto, N., 1971. Magnetic properties of synthesized titanomaghemite. J. Geophys. Res. 76, 7035–7046.

Polyak, L., Curry, W.B., Darby, D.A., Bishof, J., Cronin, T.M., 2004. Contrasting glacial/interglacial regimes in the western Arctic Ocean as exemplified by a sedimentary record from the Mendeleev Ridge. Palaeogeogr. Palaeoclimatol. Palaeoecol. 203, 73–93.

Readman, P.W., O'Reilly, W., 1970. The synthesis and inversion of non-stoichiometric titanomagnetites. Phys. Earth Planet. Inter. 4, 121–128.

Readman, P.W., O'Reilly, W., 1972. Magnetic properties of oxidized (cation deficient) titanomagnetites (Fe, Ti, □)$_3$ O$_4$. J. Geomagn. Geoelectr. 24 (1), 69–90.

Roberts, A.P., Winklhofer, M., 2004. Why are geomagnetic excursions not always recorded in sediments? Constraints from post-depositional remanent magnetization lock-in modelling. Earth Planet. Sci. Lett. 227, 345–359.

Schult, A., 1968. Self-reversal of magnetization and chemical composition of titanomaghemites in basalts. Earth Planet. Sci. Lett. 4, 57–63.

Schult, A., 1971. On the strength of exchange interactions in titanomagnetite and its relation to self-reversal of magnetization. Zeitschrift für Geophysik 37, 357–365.

Soubrand-Colin, M., Horan, H., Courtin-Nomade, A., 2009. Mineralogical and magnetic characterization of iron titanium oxides in soils developed on two various basaltic rocks under temperate climate. Geoderma 149, 27–32.

Spielhagen, R.F., Baumann, K.H., Erlenkeuser, H., Nowaczyk, N.R., Nøorgaard-Pedersen, N., Vogt, C., Weiel, D., 2004. Arctic Ocean deep-sea record of northern Eurasian ice sheet history. Quat. Sci. Rev. 23, 1455–1483.

Stein, R., Schubert, C.J., MacDonald, R.W., Fohl, K., Harvey, H.R., Weiel, D., 2003. The central Arctic Ocean: distribution, sources, variability, and burial of organic carbon. In: Stein, R., MacDonald, R.W. (Eds.), The organic carbon cycle in the Arctic Ocean. Springer-Verlag, Berlin, pp. 295–314.

Steuerwald, B.A., Clark, D.L., Andrew, J.A., 1968. Magnetic stratigraphy and faunal patterns in Arctic Ocean sediments. Earth Planet. Sci. Lett. 5, 79–85.

Uyeda, S., 1958. Thermo-remanent magnetization as a medium of paleomagnetism, with special reference to reverse thermo-remanent magnetism. Jpn. J. Geophys. 2, 1–123.

Verhoogen, J., 1956. Ionic ordering and self-reversal in impure magnetites. J. Geophys. Res. 61, 201–209.

Verhoogen, J., 1962. Oxidation of iron–titanium oxides in igneous rocks. J. Geol. 70, 168–181.